

# Electronic and Optical Properties of AlN Nanosheet Under Uni-axial Strain

F. Ghasemzadeh and F. Kanjouri\*

Faculty of Physics, Kharazmi University, 31979-37551, Tehran, Iran.

(\*) Corresponding author: kanjouri@khu.ac.ir

(Received: 15 April 2017 and Accepted: 09 January 2018)

## Abstract

We have investigated the electronic and optical properties of AlN hexagonal nanosheets under different kinds of strains, using the band structure results obtained through the full potential linearized augmented plane wave method within the density functional theory. The results show that 10% uniaxial strain along the zig-zag direction induces an indirect to direct band-gap transition. The dielectric tensor and corresponding optical properties are derived within the random phase approximation. Specifically, the dielectric function, reflectivity and refractive index of AlN nanosheets are calculated for both parallel ( $E_{\parallel}$ ) and perpendicular ( $E_{\perp}$ ) electric field polarizations.

**Keywords:** 2D Nanosheet, Electronic properties, Optical properties, Strain.

## 1. INTRODUCTION

In recent years, different nanostructures such as graphene [1], MoS<sub>2</sub> [2,3], MoSe<sub>2</sub> [2], Silicene [4], ZnO [5], SiC [6], Stanene [7,8], Germanene [9] and Plumbene [10] have been studied both experimentally and theoretically. Among these materials, group-III nitride semiconductor nanostructures have drawn considerable attention for their interesting properties and promising applications in spintronics, semiconductor lasers, opto-electronics, nanoelectronics and solar cells.

AlN has a wide band gap of 6.1 eV, which is very suitable for modern electronic and optoelectronic applications [11, 12]. AlN appears in several structural forms at the nano scale, ranging from nanowires, nanotubes and nanocones to nanosheets. Among these wide arrays of nanostructures, the 2 dimensional monolayer nanosheet with a honeycomb lattice structure has drawn a great deal of research interest. Peng Liu et al. studied inducing indirect to direct transition in band gap by shear strain and dynamical stability of AlN monolayer nanosheet [13]. Tsipas P et al. report on the epitaxial growth of thin AlN films on Ag (111) substrates by plasma assisted molecular

beam epitaxy as a graphite-like hexagonal lattice [14]. Zhang [15] have investigated the electronic structures and magnetic properties of AlN nanosheets and AlN NTs. Yuting Peng et al. have investigated the p-type impurity properties in the Mg-doped AlN nanosheet by means of first-principles calculations [16]. However, variation in band structure and optical properties of AlN nanosheets under application of strain is relatively less explored. Strain is known to be very effective in manipulating the carrier mobility, electronic and band structure in nano materials.

In this work we have calculated electronic structure and optical properties of AlN under different degrees and types of strain within the framework of density functional theory (DFT).

## 2. COMPUTATIONAL METHOD

All calculations presented in this work are based on DFT using all the electrons and full potential code WIEN2k. In order to achieve energy eigenvalues convergence, the wave function in the interstitial region was expanded in terms of

plane waves with a cut-off parameter of  $RMT \cdot K_{max} = 6.0$ , where  $RMT$  denotes the smallest atomic sphere radius and  $K_{max}$  denotes largest  $k$  vector in the plane wave expansion. For the exchange-correlation energy functional, in order to treat electron exchange-correlation, we choose the Perdew – Burke - Ernzerhof (PBE) formulation of the GGA, which yields the correct ground-state structure of the combined systems. Magnitude of the largest vector in charge density Fourier expansion or the plane wave cut-off was set to  $G_{max} = 14 \text{ Ry}^{1/2}$ . The optical spectra were calculated using 210  $k$ -points in the first Brillouin zone (BZ). Also a sufficiently large  $15 \text{ \AA}$  vacuum region was used to separate the two-dimensional structures to rule out any interaction among the neighboring layers along  $z$ -axis.

### 3. RESULTS and DISCUSSION

#### 3.1. Structural and Electronic Properties

We have studied the rectangular unit cell which is shown in Fig.1. Since the rectangular structure has two non-equivalent direction we have studied two different modes of strain (a) uniaxial strain along the  $x$  axis (i.e. zig-zag direction); (b) uniaxial strain along the  $y$  axis (i.e. arm-chair direction). The different values of compressive and tensile strain are considered as follows:

$$\frac{a_{eq} - a_{\varepsilon}}{a_{eq}} \times 100 = \pm \varepsilon \quad (1)$$

where  $\varepsilon = 0, 5$  and  $10$ ,  $a_{eq}$  is the free-strain lattice constant and the positive and negative signs refer to compressive and tensile strains, respectively.

The hexagonal nanostructure of AlN is first optimized by the conjugated gradient method. The Al-N bond length is obtained  $1.83 \text{ \AA}$ , which is very close to previous theoretical calculations and in a good agreement with experimental ones [17, 18, 20].

The total density of states of AlN nanosheet versus energy of electrons in

monolayer under different uniaxial strain along the  $x$  and  $y$  axes are shown in Fig.2.

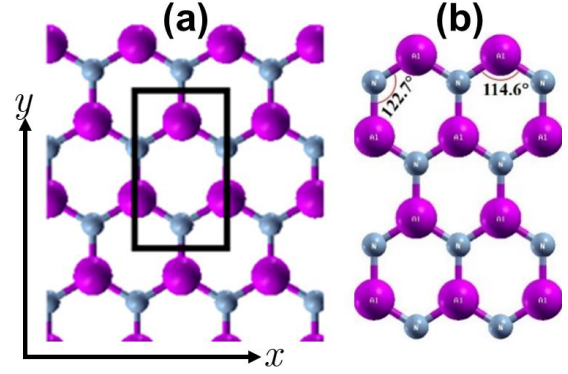


**Figure 1.** (a) Illustrates AlN 2D monolayer structure in strain free condition. The black rectangle-shape denote to the considered unit cell in our calculations. [purple ball: Al atom, blue ball: N atom]. (b) AlN 2D monolayer under 10% strain along zig-zag direction. (For interpretation of the references to color in this figure legend, the reader is referred to the web version of this article.)

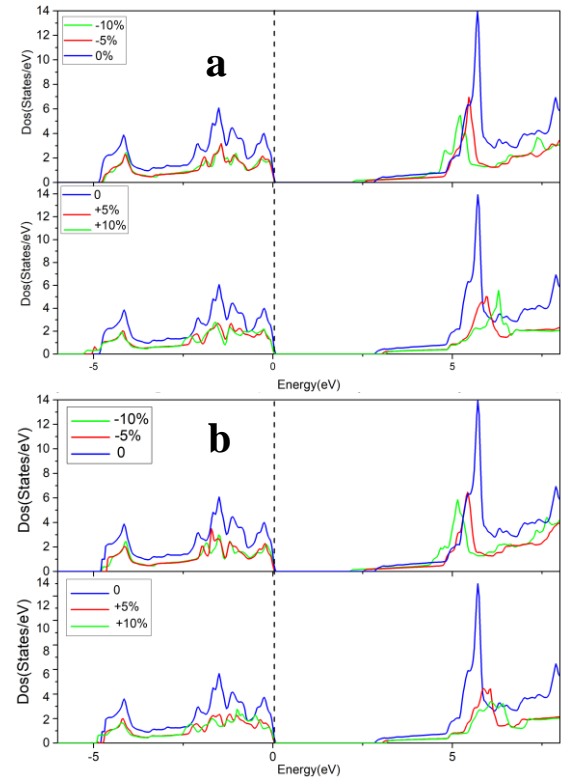


**Figure 2.** Total density of states for (a) under uniaxial strain along zig-zag direction and (b) under uniaxial strain along arm-chair direction.

Under compressive uniaxial strain along the x(y) axis, AlN monolayer has got larger energy band gaps than strain-free monolayer, while it has got smaller energy band gap than strain-free condition under tensile uniaxial strain along x(y) axis. The exact value of energy band gap has been listed in Table 1.

**Table 1.** Calculated electronic band gap.

$E_g$ (eV)	-10%	-5%	0	5%	10%
$E_g(\parallel x)$	2.25	2.58	2.88	3.06	3.18
$E_g(\parallel y)$	2.16	2.56	2.88	3.09	3.20

values (eV).

Also, our band structure calculations show that AlN nanosheet is a semiconductor with an indirect band gap of 2.88eV that is in a good agreement with previous theoretical results [19,20]. Fig. 3 illustrates the variation of band gap of AlN nanosheet under uniaxial strains from -10% to 10% for both zig-zag and arm-chair directions. As can be seen in this figure the magnitude of band gap increases with the uniaxial strain, when strain is increased from -10% to 10%. There is an indirect to direct band gap (3.18eV) transition at 10% uniaxial strain along the zig-zag.

### 3.2. Optical Properties

The optical properties of AlN nanosheet such as real and imaginary parts of dielectric tensor, reflectivity and refractive index for both parallel and perpendicular polarization of electric field vector are calculated.

For perpendicular polarization, the direction of the electric field is chosen to be incident perpendicular to the plane of the AlN nanosheet, whereas for parallel polarization, it is chosen to be parallel to the plane of the AlN nanosheet.

Optical calculations are performed in the random phase approximation (RPA) by using Wien2k code. The optical properties can be gained from the complex dielectric

function  $\varepsilon(\omega)$  to describe the optical response of the medium to the electromagnetic field at all energies:

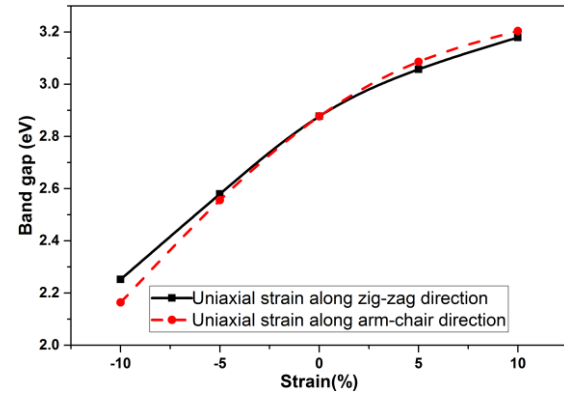


**Figure 3.** Band gap versus strain for AlN nanosheet in rectangular unit cell. Filled and unfilled symbols represent the indirect and direct band gaps, respectively.

$$\varepsilon(\omega) = \varepsilon_1(\omega) + i\varepsilon_2(\omega) \quad (2)$$

where  $\varepsilon_1(\omega)$  and  $\varepsilon_2(\omega)$  are real and imaginary parts of complex dielectric function respectively. There are two contributions to  $\varepsilon(\omega)$ , namely, interband and intraband transitions which involve scattering of photons and are expected to give a small contribution to  $\varepsilon(\omega)$ .

The imaginary part of the dielectric function  $\varepsilon_2(\omega)$  is given by [21]:

$$\varepsilon_2(\omega) = \frac{ve^2}{2\pi\hbar m^2 \omega^2} \int d^3k \sum_{kk'} \left[ \frac{|\langle kn | \mathbf{P} | kn' \rangle|^2 f(kn)(1 - f(kn'))}{\delta(E_{nk} - E_{n'k} - \hbar\omega)} \right] \quad (3)$$

where  $\hbar\omega$  is the energy of the incident photon,  $\mathbf{P}$  is the momentum operator,  $\frac{\hbar}{i} \frac{\partial}{\partial x'}$ ,  $|kn\rangle$  is the eigenfunction with eigenvalue  $E_{nk}$  and  $f(kn)$  is the Fermi distribution function. The real part of the dielectric function  $\varepsilon_1(\omega)$  follows from the Kramers-Kronig relation:

$$\varepsilon_1(\omega) = 1 + \frac{2}{\pi} \mathbf{P} \int_0^\infty \frac{\varepsilon_2(\omega') \omega' d\omega'}{\omega'^2 - \omega^2} \quad (4)$$

where  $\mathbf{P}$  stands for the principal value of the integral over  $\omega'$ .

We have calculated optical properties of AlN nanosheet for both parallel ( $E_{\parallel}$ ) and

perpendicular ( $E_{\perp}$ ) electric field polarizations. For these directions of electric field, real and imaginary parts of dielectric function are shown in Fig.4 and Fig.5.

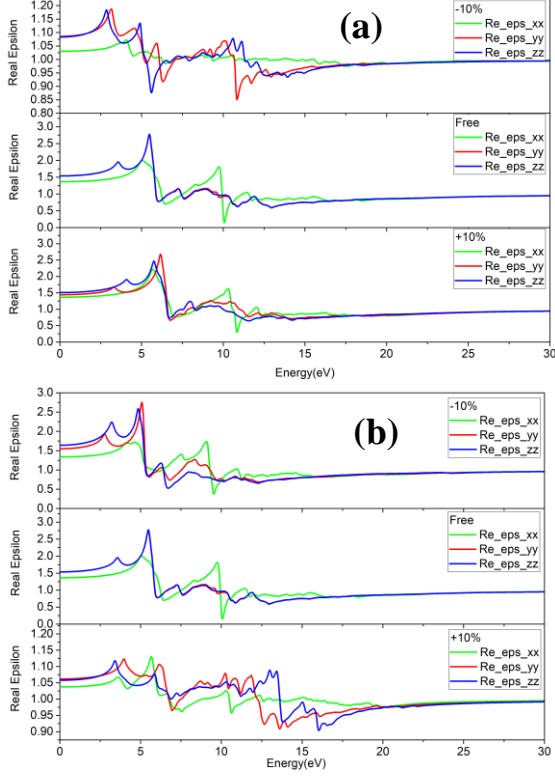


**Figure 4.** Real parts of dielectric function of AlN nanosheet in different directions for (a) under uniaxial strain along zig-zag direction and (b) under uniaxial strain along arm-chair direction.

The static value of the real part of the dielectric function ( $\epsilon_1(0)$ ) for AlN in strain-free condition is respectively given as 1.54 and 1.36 for  $E_{\parallel}$  and  $E_{\perp}$ . Under uniaxial strain along zig-zag direction  $\epsilon_1(0)$  for both parallel directions  $\epsilon_{\parallel(x)}$  and  $\epsilon_{\parallel(y)}$  have the same values and are different from perpendicular ones ( $\epsilon_{\perp(z)}$ ). While Under uniaxial strain along arm-chair direction straining structure can cause an impalpable effect on the value of static dielectric constant in parallel polarization. We have also calculated the static dielectric constant  $\epsilon_1(0)$  for AlN nanosheet under different kind of uniaxial strain along zig-zag and arm-chair

directions that have been reported in Table 2.

The refractive index of AlN nanosheet that has been calculated according to Eq. (5) is depicted versus energy for both polarizations under different kinds of uniaxial strain.

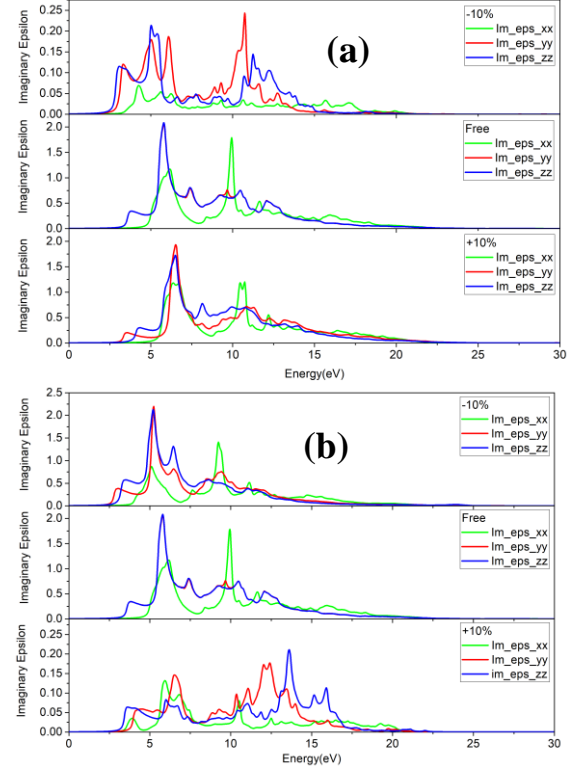


**Figure 5.** Imaginary parts of dielectric function of AlN nanosheet in different directions for (a) under uniaxial strain along zig-zag direction and (b) under uniaxial strain along arm-chair direction.

The refraction spectrum for -10%, 0 and +10% cases are plotted in the terms of incident photon energy in Fig. 6.

$$n(\omega) = \left( \frac{\sqrt{\epsilon_1^2 + \epsilon_2^2} + \epsilon_1}{2} \right)^{\frac{1}{2}} \quad (5)$$

The value of static refractive index in strain-free condition in parallel polarization ( $n_{\parallel}(0)$ ) is 1.24; while its value in perpendicular polarization is 1.17. The minimum value of the refractive index takes place at 10.92 eV and 10.14 eV energy in ( $E_{\parallel}$ ) and ( $E_{\perp}$ ) polarizations, respectively.

The static refractive index for both parallel  $n_{\parallel(x)}$  ( $n_{\parallel(y)}$ ) and perpendicular  $n_{\perp(z)}$  directions is seen. Also, the results exhibit that refraction spectra have the maximum value between 5-12 eV range. The static refractive index has different values along zig-zag and arm-chair directions. We have also calculated the exact values of refractive index  $n(\omega)$  for AlN nanosheet under different kind of strain that have been reported in Table 3.

**Table 2.** Dielectric constant of AlN nanosheet under different uniaxial strain.

Strain along zig-zag direction	$\epsilon_{\perp(z)}$	$\epsilon_{\parallel(y)}$	$\epsilon_{\parallel(x)}$
10	1.03	1.05	1.06
5	1.01	1.01	1.01
0	1.36	1.54	1.54
-5	1.02	1.07	1.07
-10	1.02	1.08	1.08
Strain along arm-chair direction			
10	1.03	1.06	1.05
5	1.33	1.52	1.47
0	1.36	1.54	1.54
-5	1.32	1.52	1.56
-10	1.30	1.53	1.62

#### 4. CONCLUSION

We have calculated the electronic structure and optical properties of AlN nanosheet with rectangular unit cell by DFT in the generalized gradient approximation. To investigate the optical properties of AlN nanosheet, the parallel ( $E_{\parallel}$ ) and perpendicular ( $E_{\perp}$ ) electric fields with respect to the AlN nanosheet are considered. It's found that the optical spectra are anisotropic along with these two polarizations. We found that the static dielectric constant for the ( $E_{\parallel}$ ) and ( $E_{\perp}$ ) doesn't have a significant difference. There are two main peaks in the imaginary parts of dielectric function along the ( $E_{\parallel}$ ) and ( $E_{\perp}$ ) and some weak peak is observed between these two peaks that are related to weak resonances. Under different strain the dielectric constant along zig-zag direction nearly is same but in arm-chair direction

changes smoothly and the refractive index in both direction changes smoothly.

**Table 3.** Refractive index of AlN nanosheet under different uniaxial strain.

Strain along zig-zag direction	$n_{\perp(z)}$	$n_{\parallel(y)}$	$n_{\parallel(x)}$
10	1.02	1.03	1.01
5	1.00	1.00	1.01
0	1.17	1.24	1.24
-5	1.01	1.03	1.03
-10	1.01	1.04	1.04
Strain along arm-chair direction			
10	1.02	1.03	1.02
5	1.15	1.23	1.21
0	1.17	1.24	1.24
-5	1.15	1.23	1.25
-10	1.14	1.24	1.27

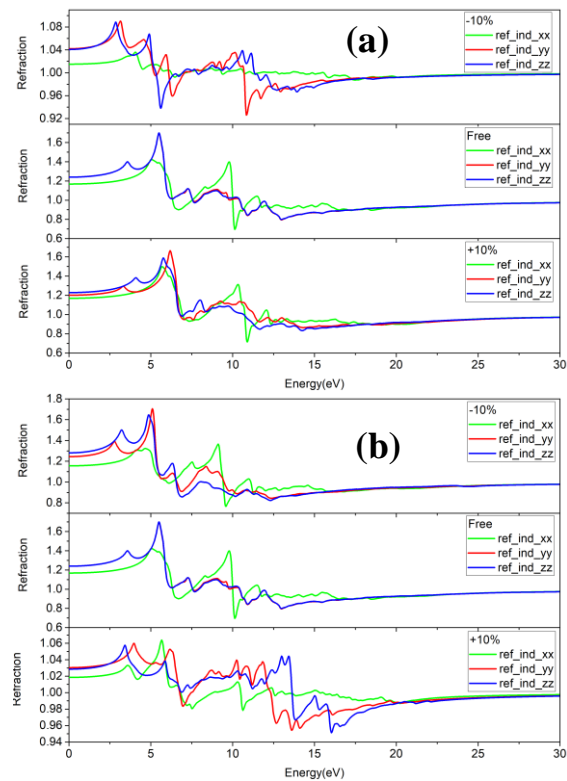


**Figure 6.** Refraction of AlN nanosheet in different directions for (a) under uniaxial strain along zig-zag direction and (b) under uniaxial strain along arm-chair.

## REFERENCES

1. Geim, A. K., Novoselov, K. S., (2007). "The rise of graphene", *Nat. Mater.*, 6 (3): 183-191.
2. Ataca, C., Şahin, H., Aktürk, E., Ciraci, S., (2011). "Mechanical and Electronic Properties of MoS<sub>2</sub> Nanoribbons and Their Defects", *J. Phys. Chem. C*, 115 (10): 3934-3941.
3. Kumar, Ashok, Ahluwalia, P. K., (2013). "Mechanical strain dependent electronic and dielectric properties of two-dimensional honeycomb structures of MoX<sub>2</sub> (X=S, Se, Te)", *Physica B: Condensed Matter*, 419: 66-75.
4. Mohan, Brij, Kumar, Ashok, Ahluwalia, P. K., (2013). "A first principle calculation of electronic and dielectric properties of electrically gated low-buckled mono and bilayer silicene", *Physica E: Low-dimensional Systems and Nanostructures*, 53: 233-239.
5. Wan, Q., Xiong, Zh., Dai, J., Rao, J., Jiang, F., (2008). "First-principles study of Ag-based p-type doping difficulty in ZnO", *Optical Material*, 30 (6): 817-821.
6. Sun, Lian, Li, Yafei, Li, Zhenyu, Li, Qunxiang, Zhou, Zhen, Chen, Zhongfang, Yang, Jinlong, Hou, J. G., (2008). "Electronic structures of SiC nanoribbons", *J. Chem. Phys.*, 129 (17): 174114-174117.
7. Zhang, Run-Wu, Zhang, Chang-Wen, Ji, Wei-Xiao, Li, Sheng-Shi, Hu, Shu-Jun, Yan, Shi-Shen, Li, Ping, Wang, Pei-Ji, Li, Feng, (2015). "Ethyne-functionalized stanene film: a promising candidate as large-gap quantum spin Hall insulator", *New Journal of Physics*, 17: 083036.
8. Wang Ya-ping, Ji Wei-xiao, Zhang Chang-wen, Li Ping, Li Feng, Wang Pei-ji, Li Sheng-shi, Yan Shi-shen, (2016). "Large-gap quantum spin Hall state in functionalized dumbbell stanene", *Applied Physics Letters*, 108: 073104.
9. Zhang Runwu, Ji Weixiao, Zhang Chang-wen, Li Shengshi, Li Ping, Wang Peiji, (2016). "New Family of Room Temperature Quantum Spin Hall Insulators in Two-Dimensional Germanene films", *J. Mater. Chem. C*, 4: 2088-2094.
10. Zhao Hui, Zhang Chang-wen, Ji Wei-xiao, Zhang Run-wu, Li Sheng-shi, Yan Shi-shen, Zhang Bao-min, Li Ping, Wang Pei-ji, (2016). "Unexpected Giant-Gap Quantum Spin Hall Insulator in Chemically Decorated Plumbene Monolayer", *Scientific Reports*, 6: 20152.
11. Vurgaftman, I., Meyer, J. R., (2003). "Band parameters for nitrogen-containing semiconductors" *J. Appl. Phys.*, 94: 3675.
12. Wu, J., (2009). "When group-III nitrides go infrared: New properties and perspectives", *J. Appl. Phys.*, 106: 011101.
13. Tsiapas, P, Kassavetis S, Tsoutsou D, Xenogiannopoulou E, Golias E, Giamini S. A., Grazianetti C, Chiappe D, Molle A, Fanciulli M, Dimoulas A, (2013). "Evidence for graphite-like hexagonal AlN nanosheets epitaxially grown on single crystal Ag (111)", *Appl. Phys. Lett.*, 103: 251605.
14. Liu, P, Sarkar, A De, Ahuja, R, (2014). "Shear strain induced indirect to direct transition in band gap in AlN monolayer nanosheet", *Computational Materials Science*, 86: 206210.
15. Shi Changmin, Qin Hongwei, Zhang Yongjia, Hu Jifan, Ju Lin, (2014). "Magnetic properties of transition metal doped AlN nanosheet: First-principle studies", *Journal of Applied Physics*, 115: 053907.
16. Peng Yuting, Xia Congxin, Zhang Heng, Wang Tianxing, Wei Shuyi, Jia Yu, (2014). "Tunable electronic structures of p-type Mg doping in AlN nanosheet", *Journal of Applied Physics*, 116: 044306.
17. Strite, S., Morkoc, H., (1992). "GaN, AlN, and InN: A review", *Journal of Vacuum Science and Technology B*, 10 (4): 1237.
18. Sahin, H., Cahangirov, S., Topsakal, M., Bekaroglu, E., Akturk, E., Senger, R., Ciraci, S., (2009). "Monolayer honeycomb structures of group-IV elements and III-V binary compounds: First-principles calculations", *Phys. Rev. B*, 80 (15): 155453-155464.
19. Liu, P., Sarkar, A., Ahuja, R., (2013). "Shear strain induced indirect to direct transition in band gap in AlN monolayer nanosheet", *Computational Materials Science*, 86: 206-210.
20. Zhang, Ch., Wang, P., (2011). "Tuning electronic and magnetic properties of AlN nanosheets with hydrogen and fluorine: First-principles prediction", *Physics Letters A*, 375 (41): 3583-3587.
21. Wooten, F., (1972). "Optical Properties of Solids", New York: University of California, Academic Press.